Mexico City Basin Effects: Past, present and future

Domniki Asimaki, Ph.D., M. ASCE[1] Juan Mayoral Villa, Ph.D.,[2] Peyman Ayoubi,[1] Kevin Franke, Ph.D., P.E., M. ASCE[3] and Tara Hutchinson Ph.D., P.E., M.ASCE[4]

[1]California Institute of Technology, Department of Mechanical and Civil Engineering, 1200 E. California Blvd., Pasadena CA 91125; e-mail: domniki@caltech.edu
[2] Instituto de Ingeniería de la UNAM, Department of Civil Engineering, Mexico City, Mexico; e-mail: JMayoralV@iingen.unam.mx
[3] Brigham Young University, Department of Civil and Environmental Engineering, 368 Clyde Building, Provo, UT 84602; e-mail: kfranke@et.byu.edu
[4] Jacobs School of Engineering, University of California, San Diego, 9500 Gilman Drive, La Jolla, CA 92093-0403; e-mail: tahutchinson@ucsd.edu

ABSTRACT

Seismic hazard in Mexico City governed by site effects. The M8.1 1985 subduction zone earthquake, which caused significant damage and loss of thousands of lives at 350km epicentral distance, has become the quintessential example of the role that site effects can play in modifying the amplitude, frequency and duration of ground shaking; and in aggravating the catastrophic consequences of earthquakes. We here present observations and analyses of the M7.1 September 19, 2017 event that --while triggered by an intraplate rupture at approximately half the epicentral distance of the 1985 event relative to Mexico City-- caused severe structural damage to a few tens of buildings located in a relatively narrow zone between the hill and lake zones of the basin, known as the transition zone. We show that the M 7.1 mainshock exposed the vulnerabilities of the pre-1985 building code in the transition zone; but more importantly highlighted the improvement of the 1987 building code revision in terms of the performance of modern high-rise buildings that suffered catastrophic consequences during the 1985 Michoácan earthquake sequence. We next analyze several records collected at stations in the basin over the past 20 years. We highlight the importance of three-dimensional heterogeneity of the basin sediments, the coupling between hydrological setting and site response and their evolution with time, and the energy interaction between the deep basin edge and the shallow clay layers. Results presented are the collective effort of the GEER teams that were deployed to perform post-earthquake reconnaissance in the affected regions of the epicentral area and in Mexico City after the M 7.1 September 19, 2017 earthquake sequence.

INTRODUCTION

At 1:14:40 p.m. local time (at 18:14:40 GMT), a moment magnitude M 7.1 earthquake struck just south of Puebla, Mexico, and 120 km SE from Mexico City, where almost 9 million people reside. According to the USGS, severe shaking was felt close to the epicenter; Mexico City experienced moderate to strong shaking, enough to cause significant structural damage. The

earthquake occurred in the complex region of normal and reverse faults with a regional tectonic mechanism associated with the subduction of the Cocos plate under the North American plate. The focal mechanism was normal faulting. The strike of the rupture plane was approximately 112 degrees and dipped to the north or south at about 42 degrees. The epicenter was located 12 km southeast of the city of Axochiapan in the state of Morelos. The epicenter of the September 19, 2017 intraplate mainshock at a depth of 57 km (Figure 1a).

Notably, the September 19 event was preceded by an M 8.2 earthquake on September 7, 2017, with epicenter in the Tehuantepec Gulf at 133 km SE of Pijijiapan in the Chiapas state. The epicenter was at 14.85 N and -94.11 W at a depth of 58 km, according to the National Seismological Service of Mexico (Servicio Sismológico Nacional, or SSN).

The September 7th earthquake caused major damage to houses in the states of Oaxaca and Chiapas. Early hypotheses that the September 7th event could have triggered the September 19th event have been disproven (source: Temblor.net). The location of the epicenters of the two events relative to the most important subduction zone events since the 1950's is depicted in Figure 1b. Ironically, this earthquake comes on the 32nd anniversary of a deadly M=8.1 Michoacán earthquake that struck 350 km SW of Mexico City, resulted in 10,000 casualties and caused billions of dollars in damage.

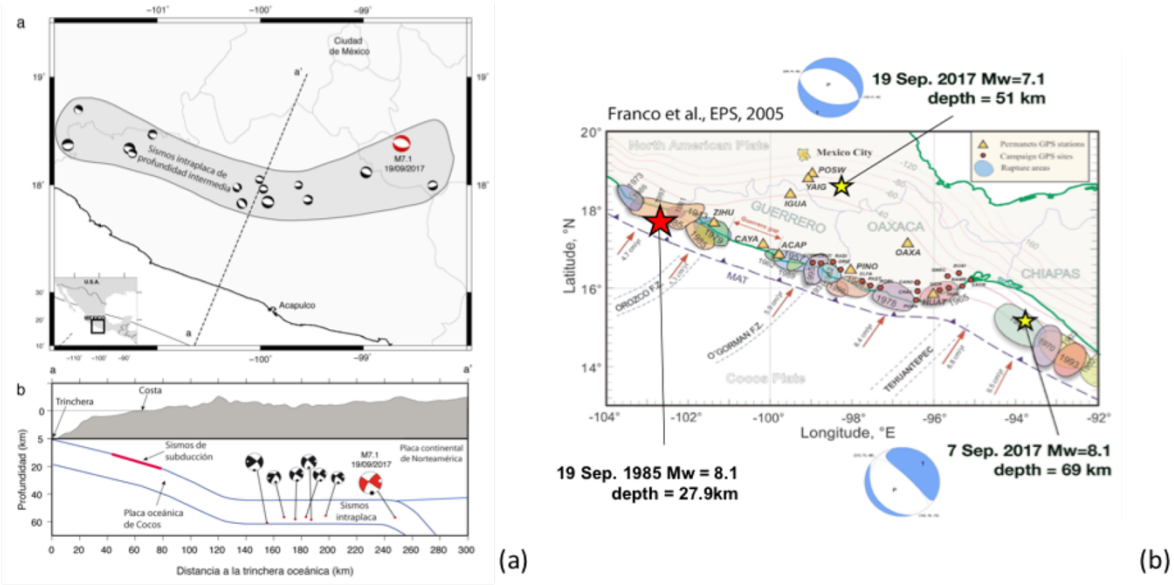

Figure 1. a) Locations of the magnitude 7.1 earthquake of September 19, 2017 (red) and some others of the same type in the region. The "beach balls" illustrate the orientation of the faults; b) Modified from Franco et al. (2005), this figure shows the location of the two intraplate events that occurred within the subducting Cocos Plate in September, 2017. Additionally, it shows the rupture areas of other large historic earthquakes in the country, including the 1985 M 8.1 Michoacán earthquake (Source: Temblor.net).

Mexico has a long history of intermediate-depth, normal-faulting earthquakes within the Cocos plate. Examples include the 1931 M7.8 earthquake that had catastrophic consequences in Oaxaca (Singh et al. 1985), the 1957 M7.7 earthquake that caused damage in Michoacán and Mexico City (Singh et al. 1996), the 1980 M7.0 earthquake which devastated Huajuapan de León in Oaxaca (Yamamoto et al. 1984), and the M7.0 earthquake of 1999 which resulted in many

damaged adobe dwellings in the region close to the epicenter and damaged colonial structures in the city of Puebla (Singh et al. 1999; Yamamoto et al. 2002). We should note here that the latest building code of Mexico City explicitly incorporates such intermediate-depth normal-faulting events when estimating the seismic hazard (Rosenblueth et al. 1989). More recently, several studies have proposed ground motion prediction models specifically aimed at estimating ground motion intensities caused by intermediate-depth normal-faulting events within the Cocos plate in Mexico (García et al. 2004, 2005; Ordaz and Singh 1992; Pacheco and Singh 1995).

Figure 1a also shows the epicenters and depths of normal-faulting earthquakes that have occurred in the last 40-50 years. Ruptures of these events occur at depths greater than typical subduction earthquakes (such as the M8.1 1985 Michoacán mainshock), which take place under the coasts of the Mexican Pacific, at the interface between the Cocos and North America tectonic plates (red line, Figure 1). Intraplate earthquakes of intermediate depth, by contrast, are produced by extension stresses along the Cocos plate. Mexico has a long history of similar intermediate-depth, normal-faulting earthquakes within the Cocos plate. Examples include the 1931 M7.8 earthquake that had catastrophic consequences in Oaxaca (Singh et al, 1985), the 1957 M7.8 earthquake that caused damage in Michoacán and Mexico City (Singh et al, 1989), the 1980 M7.1 earthquake which devastated Huajuapan de León in Oaxaca (Yamamoto et al, 1984), and the M7.0 earthquake of 1999 which resulted in many damaged adobe dwellings in the region close to the epicenter and damaged colonial structures in the city of Puebla (Singh et al, 1999; Yamamoto et al,).

According to García et al (2005), the probability of ground shaking in Mexico City caused by intraplate earthquakes is similar to that caused by subduction earthquakes, such as that of 1985, among others. In other words, the seismic hazard in Mexico's capital is equally controlled by intraplate earthquakes and by subduction earthquakes that occur under the coast of the Mexican Pacific. We should also mention here that intraplate normal-faulting events were explicitly included in the revised (post-1985) building code of Mexico when estimating the seismic hazard for infrastructure design and risk assessment (Rosenbluth et al, 1989); while several more recent studies have proposed ground motion prediction models developed specifically to estimate ground motion intensities caused by intraplate normal-faulting events within the Cocos plate in Mexico (García et al, 2005).

SEISMIC GEOZONATION AND STRONG MOTION STATIONS

Figure 2 depicts the areas where sedimentary deposits govern the seismic hazard of the basin – the seismic geo-zonation of Mexico City: Zone II indicated by yellow, and Zone III by the orange, brown and red shaded areas. Zone III been subdivided into Zones IIIa, IIIb, IIIc and IIId (orange, brown, red and deep red accordingly) to account for the increasing depth of the clay deposits when moving from the hill zones to the center of the old lakes.

Site conditions in Zone II, referred to as the Transition Zone, are characterized by soft clay deposits interbedded by series of thin silty sand and sandy silt layers and lenses, which range in thickness from 0-20 m. These layers are underlain by stiffer sandy silt and silty sand deposits, with interbedded clay layers of varying thickness ranging from a few tens of centimeters to meters.

The typical soil profile for Zone III (Lake Zone), includes a 1-2m thick desiccated clay crust underlain by a soft to very soft clay layer approximately 25 to 35 m thick, with thin interbedded lenses of sandy silts and silty sands. Below the upper soft clay lies a layer of very

dense sandy silt (4 to 7 m thick), which rests on a stiff clay deposit 50 to 60 m thick, itself interlaced by very dense sandy silt and silty sands lenses. At larger depths lies a competent layer of very stiff to hard sandy silt and silty clay. For more information, interested readers are referred to Auvinet et al. (2011) and Mayoral et al. (2016).

Various organizations were operating and maintaining ground motion recording instruments at the time of the September 19th event. Among others, Centro de Instrumentación y Registro Sísmico (CIRES) was operating 53 strong motion stations at the time of the event, Red Acelerográfica de Movimientos Fuertes del Instituto de Ingeniería (IINGEN) at UNAM was operating 18 stations, and the Servicio Sismológico Nacional (SSN) del Instituto de Geofísica (IGEOF) of UNAM was operating 10 stations. Figure 2 also depicts the locations of stations where ground motions were made available to the UNAM-GEER team in the Mexico City Basin.

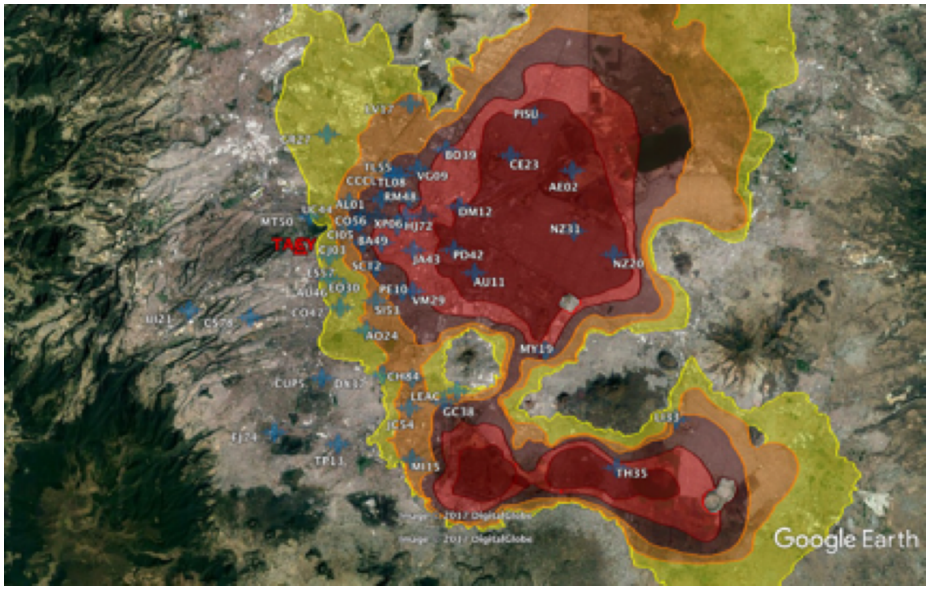

Figure 2. II-UNAM and CIRES strong ground motion stations active during the 2017 Puebla Mexico City earthquake.

Historical macroseismic and recorded evidence suggest that the ground surface response will reveal the dominant role of site effects in determining seismic hazard, particularly pertaining to the shallow slope of the dipping layer (transition zone between the hill and the lake zones) and to the strong impedance contrast between the shallow unconsolidated clay and the deeper sediments. At the same time, one observes considerable spatial variability in the strong motion distribution over distances of tens of meters. Figure 3 depicts the response spectra of ground motions in the vicinity of the severely stricken neighborhood of La Condesa, denoted by a dashed white rectangular in Figure 2. In this example, across a distance of less than 3 km, one can observe a shift of the response spectral peak from station ES57: 0.8 s to CI05: 1.0 s to CJ03: 2.0 s to BA49: 2.5 s. Assuming that the source and path characteristics experienced by the above stations are approximately equal; and that the recordings are not contaminated by instrument calibration errors and external effects such as soil-structure interaction, this variability in strong motion characteristics likely reflects the complex geometry of the basin edge, with spatially varying basement slope across short distances.

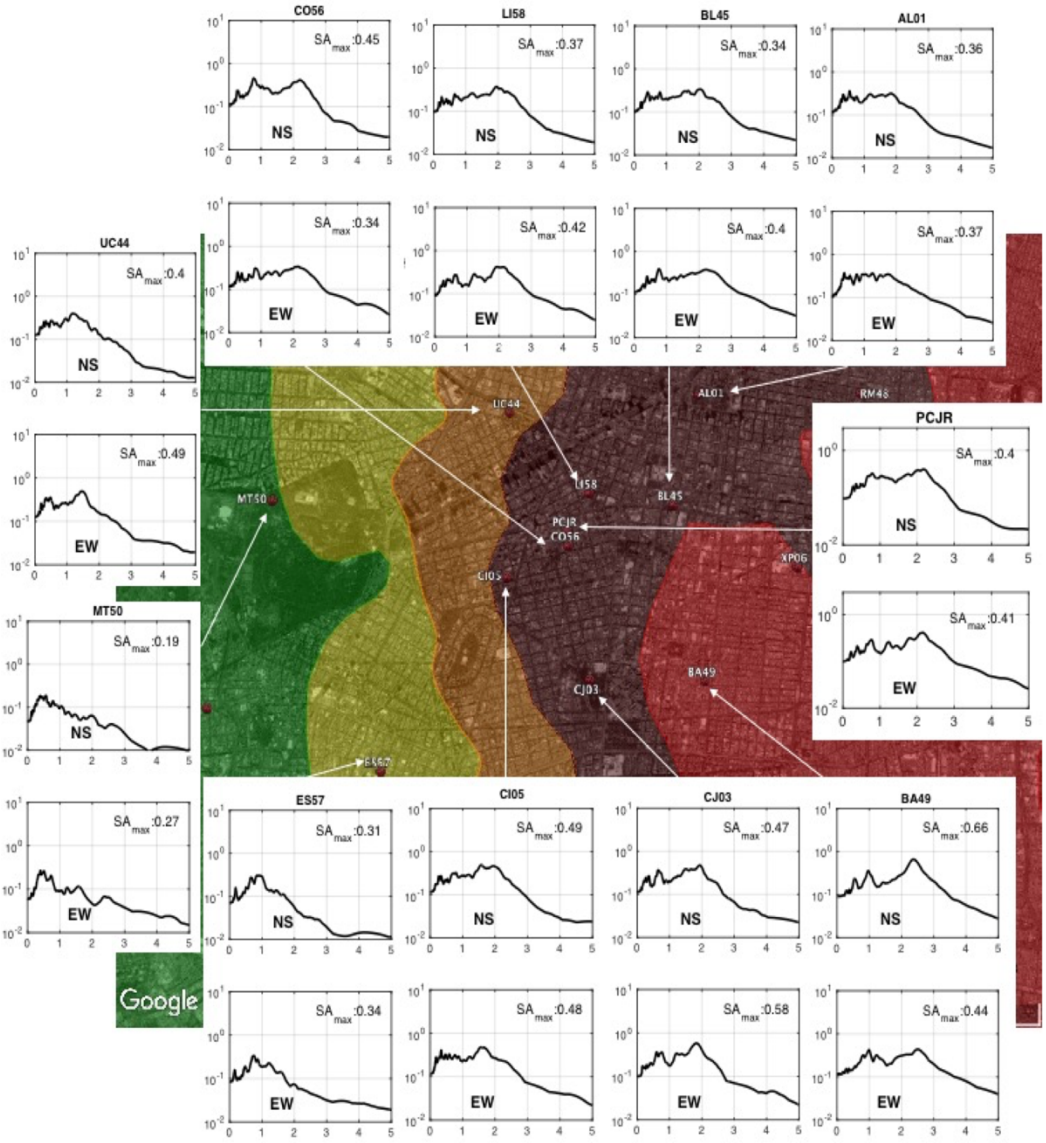

Figure 3. Spatial variability of ground shaking in the vicinity of Condesa, where extensive damage was caused to 5-10 story buildings by the 2017 M 7.1 event. Ground shaking characteristics represented by means of 5% damped elastic response spectra. Spectra plotted as a function of period T[sec].

SIMILARITIES AND DIFFERENCES BETWEEN THE 2017 AND 1985 GROUND MOTIONS AND THEIR DAMAGE CONSEQUENCES IN MEXICO CITY

The M 7.1 September 19, 2017 event was triggered by an intraplate rupture at approximately half the epicentral distance of the M 8.0 1985 event relative to Mexico City. The shorter rise time of the crustal source and smaller epicentral distance resulted in ground shaking in the hill zone that was considerably richer in high-frequencies than the 1985 event. In turn, these ground motion characteristics transpired into more significant site amplification of ground motions on the

surface of the shallower sandy silts and silty sands layers of the transition and outer lake zones; and consequently, resulted in more significant impact to shorter period structures than those affected during the 1985 earthquake.

Similar to 1985, site effects played an important role in shaping the damage distribution across the basin: the majority of severely damaged structures were concentrated within a 7 x 20 km^2 area in the west and southwest Transition Zone (II) and Lake zones IIIa and IIIb. While Zones II, IIIa and IIIb contained 85% of the high risk and 95% of the collapsed buildings (source: CICM 2017), it is important to note however that the majority of these structures (~90%, Galvis et al., 2017) were constructed prior to 1985 but lacked ample inspection/retrofit.

Thus, while reconnaissance and damage mapping efforts suggest that double resonance of site and structure led to the concentration of damage towards the North-West of the basin, the seemingly causative relationship between site effects and damage is skewed due to parameters such as construction quality, design code, material degradation from continuous seismic activity, and building to building interaction –namely factors we could not control for in aggregate. Detailed damage maps of severely damaged neighborhoods and their correlation with site response as recorded by strong motion stations or measured by non-invasive techniques by the GEER team; as well as more details on building damage statistics organized by (CICM, 2017) can be found in the UNAM-GEER Reconnaissance Report (Mayoral et al, 2017).

To demonstrate salient differences between the effects that source mechanisms and seismic energy attenuation of subduction and intraplate events have in the basin response of Mexico City, we next compare ground motions recorded on a hill and a lake zone stations during the 1985 M 8.1 Michoacán earthquake and the 2017 M 7.1 intraplate event (Figure 1b). We specifically compare the strong motion records at stations CUP and SCT (locations depicted in Figure 4), stations that were widely used to demonstrate site effects following the 1985 Michoacán earthquake. On the same figure, we also compare the strong motion stations at TACY, which we used as reference site in subsequent site response calculations. We should note here that originally, the code of the stations was CUMV and SCT1 respectively; the upgraded network instruments were renamed to CUP5 and SCT2. Since the instruments are practically co-located, and to avoid unnecessary confusion, we shall heretofore refer to records at these locations as CUP and SCT.

The recorded seismograms show that the amplitude of the seismic waves with periods of oscillation less than 2 seconds was much bigger in 2017 than in 1985 (on average about 5 times). The opposite was observed for periods greater than 2 seconds, which at the reference station CUP were shown to be up to one order of magnitude higher in 1985 compared to the corresponding record of 2017.

Preliminary evaluation of the 2017 ground motions records available to date indicate that response spectral ordinates did not exceed those of Appendix A of the 2004 code (Ordaz et al 2003) or those of the new code that was about to be published. Similarly, preliminary evaluation of some of the post-1985 structures that collapsed suggest that these structures did not comply with one or more of the requirements of the building code. Lastly, the large majority of the buildings that collapsed had one or more of the following characteristics: (1) being older pre-1985 non-ductile reinforced concrete structures; (2) having a structural lateral resisting system consisting of flat-slabs supported by reinforced concrete columns; and (3) having a soft story (Galvis et al., 2017). Also very common (in 41% of the collapsed buildings) were buildings located in block corners where effects of torsion are typically more severe (Galvis et al, 2017). All of these characteristics were also commonly observed during the 1985 earthquake. In that

sense, the difference in motion characteristics of the 2017 and 1985 events exposed similar poor construction practices, albeit at different locations across the basin, where the incoming ground shaking was amplified; and for different building heights that further resonated with the amplified ground shaking.

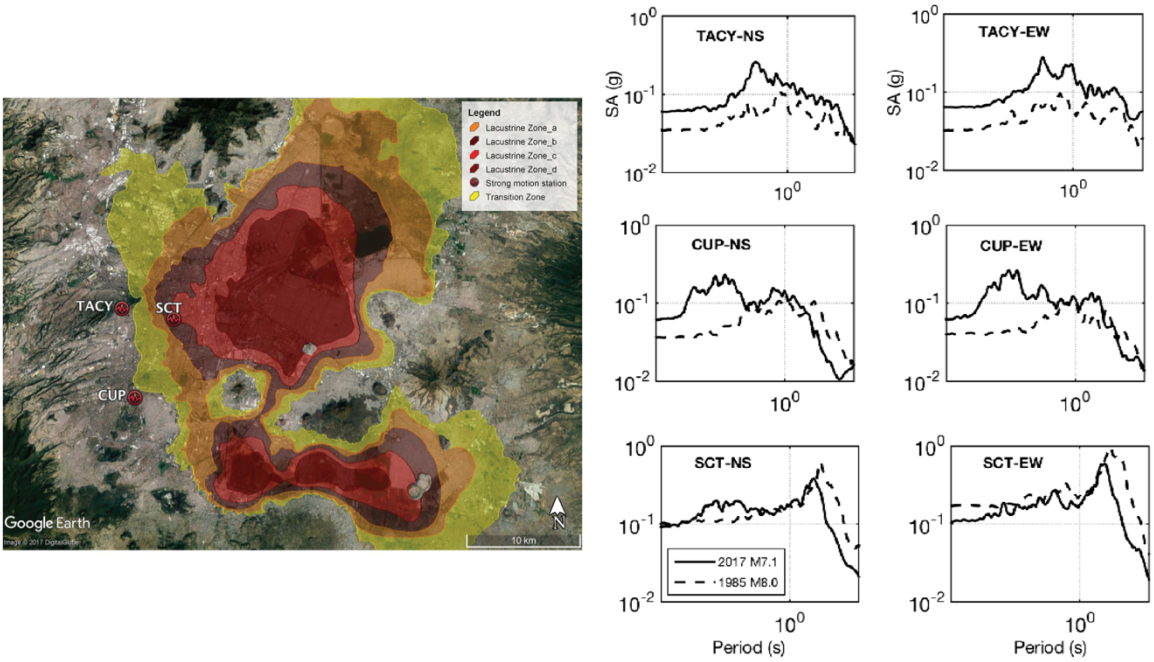

Figure 4. (left) Geotechnical zonation of the sedimentary basin underlying Mexico City. The yellow shaded contours correspond to the so-called Transition Zone, where the M 7.1 September 19, 2017 event caused most of the structural damage; (right) Comparison of the acceleration response spectra at 5% damping at reference stations CUP and TACY; and a station in the lake zone (SCT) that recorded both the 1985 M8.0 and the 2017 M 7.1 mainshocks. These stations depicted by yellow stars.

Figure 6 next plots 8 strong motion records across the basin, first broadband and then filtered each in a different frequency band (denoted in brackets). Filtering was performed using Butterworth zero phase IIR filter of fourth order. The purpose of this procedure is to reveal how different frequency characteristics are amplified in intensity and duration as they travel through the various geotechnical zones of the basin.

The frequency band 1-2 Hz (period $0.5 < T < 1$ sec) on the right, which depicts the filtered ground motions with the highest frequency content, shows that the reference station (TACY in the Hill Zone) was quite rich in high frequencies. This is expected, given the source mechanism (intraplate crustal earthquake) described above. As the incident ground motion in this frequency range propagated through the sediments, one observes systematic patterns of the effects that these specific frequency components experience: all records showed amplification compared to the record of TACY, with the maximum effects observed at the stations ES57, CJ03 and NZ20. On the same time, the records at station SCT2 and BA49, only a few hundred meters away from CI05 and in the same geoseismic zone, showed very different amplification pattern – in amplitude and duration. Perhaps this is an example supporting the hypothesis of Campillo et

al. (1989) that lateral variations of material properties may affect the variability of ground motion over very short distances due to the very low shear wave velocity of the clay deposit, but this local irregularity in the pattern requires further study.

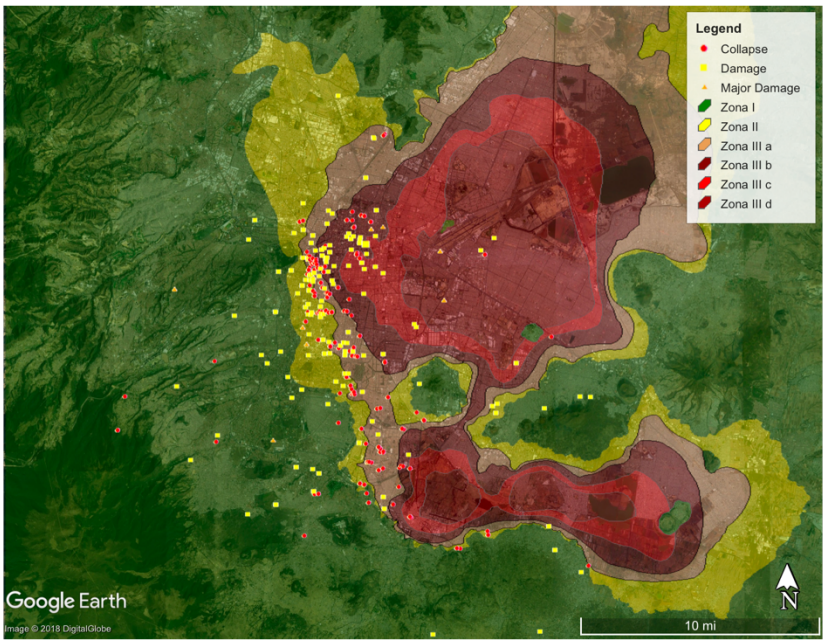

Figure 5. Collapsed buildings in the central region of Mexico City during the September, 19 1985 event and the September 19, 2017 event

Focusing next on the ground motions filtered between 0.5 – 1 Hz (period $1 < T < 2$ sec) we observe that despite the very low energy content of rock outcrop motion in these frequencies, the frequency characteristics are strongly amplified in Zone IIIb, beyond which the amplification and duration decreases. Station NZ20 in Zone IIId shows an 'unexpected' amplification pattern --very similar to stations SCT2, CJ03 and BA49 in Zone IIIb, an anomaly that may be the result of 3D effects that cannot be explained by 1D wave propagation.

Finally, although the rock outcrop motion contains very little energy at long periods, as can be seen in the ground motions filtered in the 0 - 0.5 Hz range (period $T > 2$ sec), these components are dramatically aggravated, in amplitude and duration inside the basin sediments: station ES57 in the Transition zone shows the least amplification (most likely because the shallow sediments in that zone have fundamental periods shorter than 2s), whereas all other stations located in the Lake Zone (IIIa, b, c and d) show qualitatively similar amplification, although with large variability even for stations that are approximately 1km apart (for example, CJ03 and BA49).

To summarize, despite the high frequency content of the strong motion records at the hill zone (that is, the high frequency content of the energy from the source and path), long periods are still the dominant components of the strong motion records in the lake zone. This observation appears to be in contradiction with the documented evidence that the most severely damaged buildings were located in the transition zone, and they had relatively short resonant periods (approximate estimate 0.5-1.5 s – see pertinent paper in this issue). An additional observation is that the amplification patterns are far from linear: long period components ($T > 1$ s) that are

amplified at station BA49 in Zone IIIc are strongly deamplified in the adjacent station CJ03 located approximately 2km away, in the same geoseismic zone. To put it differently, one would expect that taller structures with resonant periods longer than 2 s should have been affected as well, due to amplification patterns that most likely are related to resonant modes of the deeper basin sediments. It appears therefore that the M 7.1 mainshock exposed the vulnerabilities of the pre-1985 building code in the transition zone by inducing double resonance – of the soil column, and of the building fundamental modes. Compared to the systematic failure of 15-20 story buildings in 1985, one could argue that the 2017 event served as a validation of the 1987 building code revision in terms of the performance of modern high-rise buildings.

SITE AMPLIFICATION IN MEXICO CITY BASIN FROM SUBDUCTION AND INTRASLAB EVENTS (1985-2017)

Arroyo et al. (2013) developed a predominant period map of Mexico City using a total of 37 interface and intra-slab earthquakes ranging from M = 5-8 in the Mexican subduction zone recorded between 1985 and 2010 at approximately 100 stations in Mexico City. The predominant period was estimated using spectral acceleration amplification factors (SA) (the reference station used was not provided in the publication) and analyzing the dependence of the first site response mode over 25 years. The observed changes were attributed to the evolution of the elastic clay properties due to subsidence from excessive water pumping in Mexico City. Despite the assumptions of Arroyo et al. (2013), particularly as they pertain to the proposed evolution of dynamic soil properties due to subsidence, their results compare very well on average with the distribution of the empirical fundamental modal periods estimated using strong motion records, and the H/V and surface wave testing results obtained by the advance and main UNAM-GEER teams, as shown in Figure 7. More information can be found the UNAM-GEER Reconnaissance Report (Mayoral et al, 2017).

We next evaluated Arroyo et al. (2013) hypothesis that the empirical amplification factors indicate systematic trend of resonant period reduction, a trend which they successively used to extrapolate predominant period maps in the basin up to year 2050, assuming conditions of 1D consolidation. Our conjecture was that the trend may also reveal dependency of the dominant period with strong motion intensity and/or magnitude and distance of each event, namely nonlinear site effects.

To test this hypothesis, we used strong motion records from four intraslab earthquakes that span a period from 2000 to 2017; their epicenters relative to the Mexico City basin are shown in Figure 8a. Next, Figure 8b shows the empirical amplification factors at stations in the vicinity of the strongly hit neighborhood La Condesa, on the west side of the transition and outer lake zones. Station ES57 in the former shows no site period change for the last 17 years. Stations CI05 and CO56 in the lake IIIa zone, and less than 1 km apart shows no change in the site period, but significant change in the amplitude, an effect that could be attributed to changes in the viscosity (damping) rather than the stiffness of the soil (since the latter would also cause a shift in the resonant frequency, in addition to the amplitude). Approximately 1 km south and still in zone IIIa, station CJ03 experienced a 50% reduction in site period over 17 years; and lastly, 1km east, in zone IIIb, station BA49 experienced site period reduction 60%. The enormous variability of the site period time dependency is also indicative of variability in the hydrological setting, pumping well layout, rate of pumping and distribution of permeable sand lenses across

the basin, which likely control the consolidation and secondary compression of the Mexico City clays.

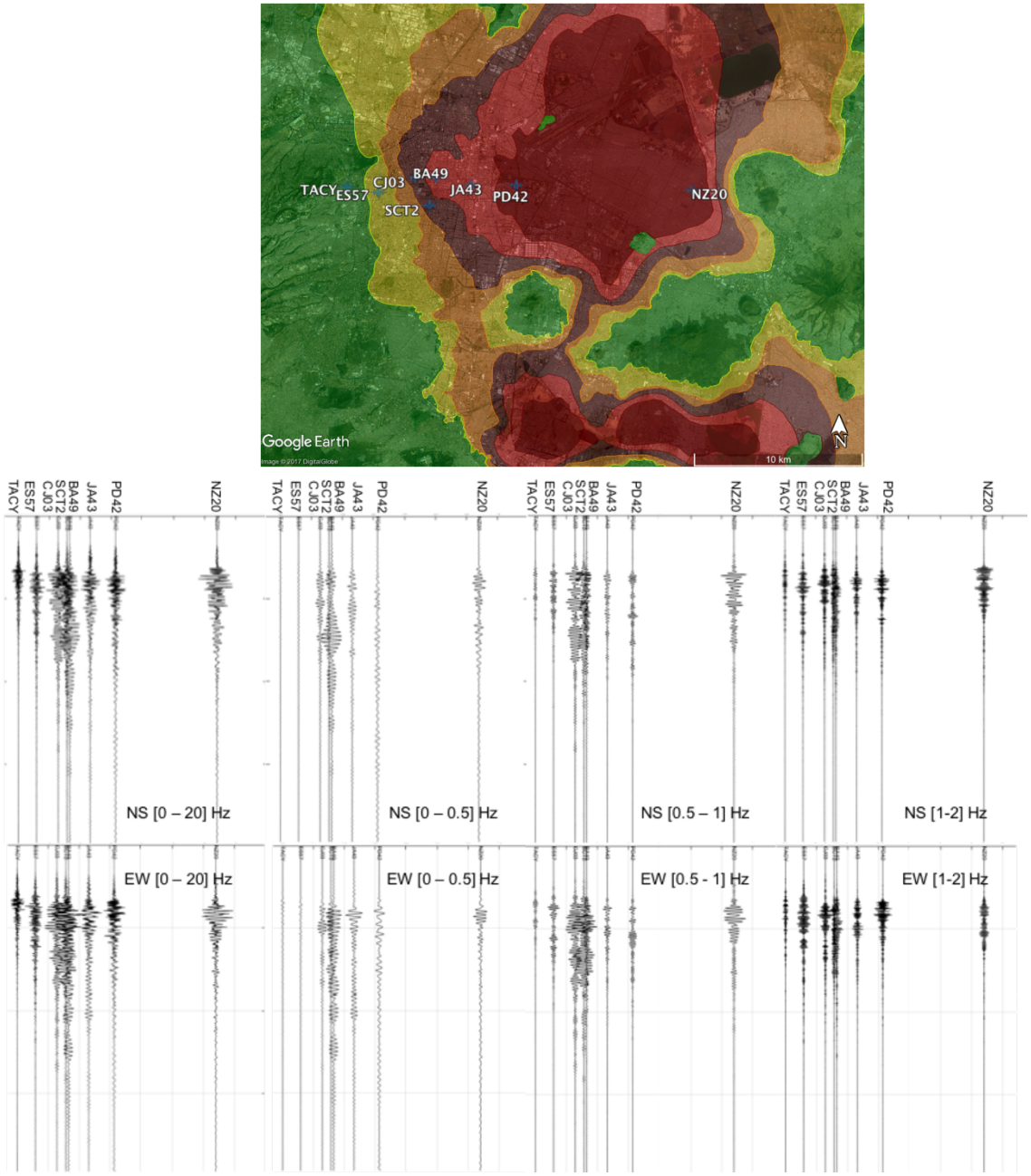

Figure 6. Broadband and filtered records of the 2017 M 7.1 mainshock from stations across the basin. From left to right in period [T sec]: Broadband, T > 2 s, 1 < T < 2 sec, and 0.5 < T < 1 sec

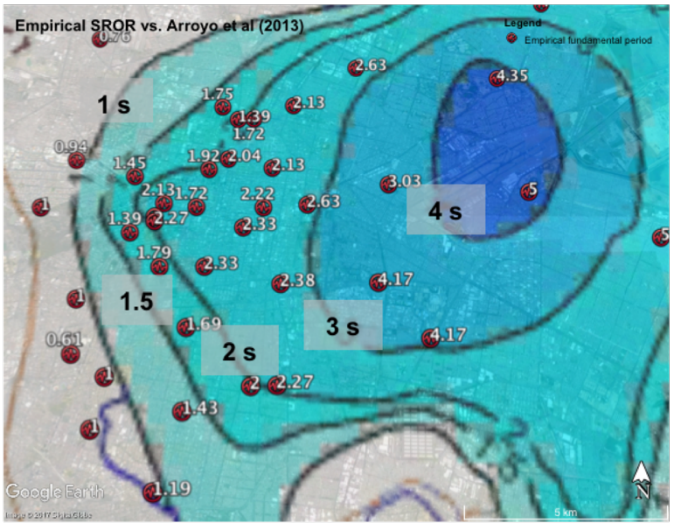

Figure 7. Empirically estimated site amplification factors using strong motion spectral ratios compared to the predominant period zonation proposed by Arroyo et al. (2013)

The amplitude of empirical surface to rock outcrop transfer functions (SROR) varies strongly between adjacent sites; and the 2000 event in some stations has substantially lower resonant frequency compared to the post-2010 events (see for example stations CJ03 and BA49 in Figure 8b). At first glance, this phenomenon could be associated with sediment consolidation over the past 20 years, namely the decrease in impedance contrast between the soft clay and underlying stiff sediments could explain, in part, the associated decrease in site response amplitude. It should be pointed out, however, that these results indicate that the shift in predominant period between 2000 and 2010 occurred only locally, suggesting that if consolidation is partially responsible for the shift, it is evidently not one-dimensional as Arroyo et al. (2013) suggested. Also, one should apply caution when interpreting modal shifts from strong motion records, because effects such as nonlinear response also manifest as shifts, sometimes irreversible, in predominant period.

Finally, we compare the strong motion spectral acceleration, empirical amplification ratios (Fourier-based, SRORs) and horizontal to vertical strong motion ratios (HVSRs) at the stations that recorded both the 1985 Michoácan and the 2017 Puebla-Mexico City events in Figure 9. As outlined in the pertinent section of this paper, the 1985 subduction zone event clearly had a much longer period content, attributed to the source rupture and Lg path of body waves from the source to the basin, several hundred kilometers away.

From a phenomenological standpoint, SRORs at stations in the lake zone could arguably be associated with nonlinear site response. In light of the results presented above, however, on the relationship between predominant site period and rapid site consolidation in Mexico City, such conclusions should be also drawn with caution, since with the information in hand, it is difficult to distinguish if the changes are due to nonlinear effects, consolidation, or a combination of the above.

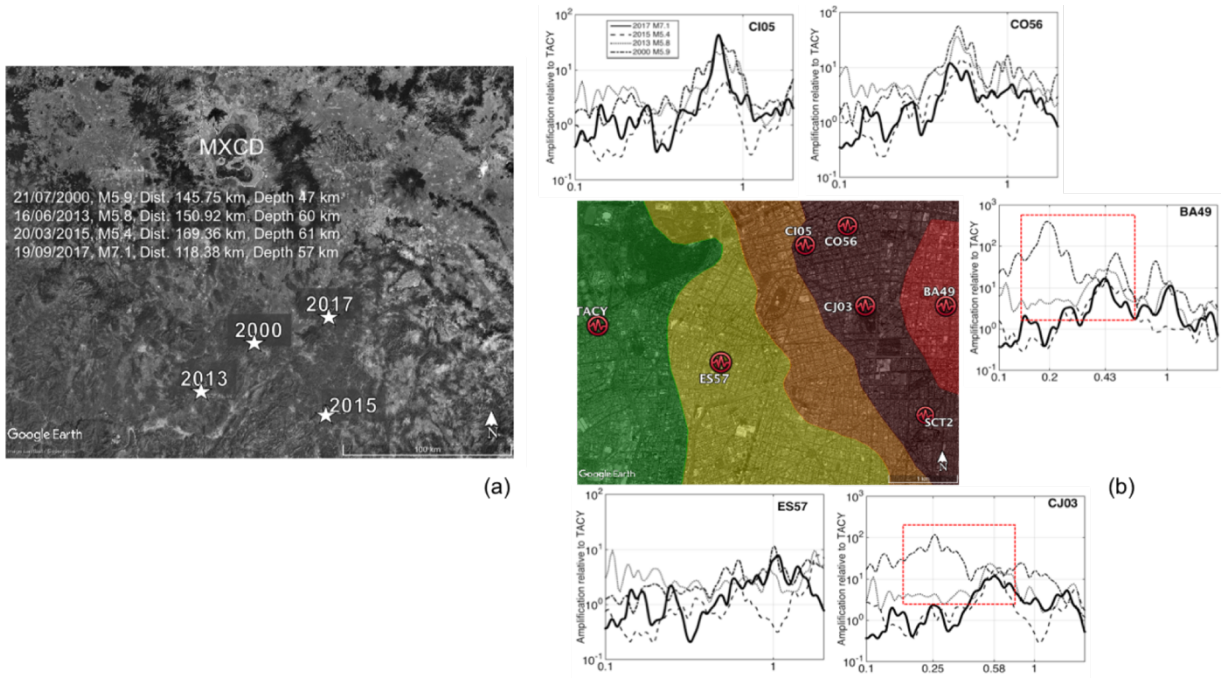

Figure 8. (a) Epicenters of the four intraslab events (2017 included) used in this section; and (b) empirical amplification factors at strong motion stations on the west side of the valley for four intraslab earthquakes. Amplification factors are shown separately for EW and NS components; and are plotted as a function of frequency [Hz].

CONCLUDING REMARKS

Our brief analysis of strong motion records recorded in Mexico City from intraslab crustal and subduction earthquakes has highlighted the importance of understanding the 2D/3D heterogeneity of the basin sediments, and the role of coupling between hydrological setting and site response. The latter is essential if we wish to capture the spatial variability of ground motion, the evolution of its properties with time and how this evolution affects the changes in the predominant period of the basin sediments. Further investigation is also needed on the subject of coupling between the shallow clay layers with the deeper sediments that was most recently discussed in Cruz-Atienza et al (2016), to understand the energy interaction between the deep basin edge and the shallow clay 'energy trap' and its role in the amplification and elongation of strong motions in the transition and outskirts of the lake zone.

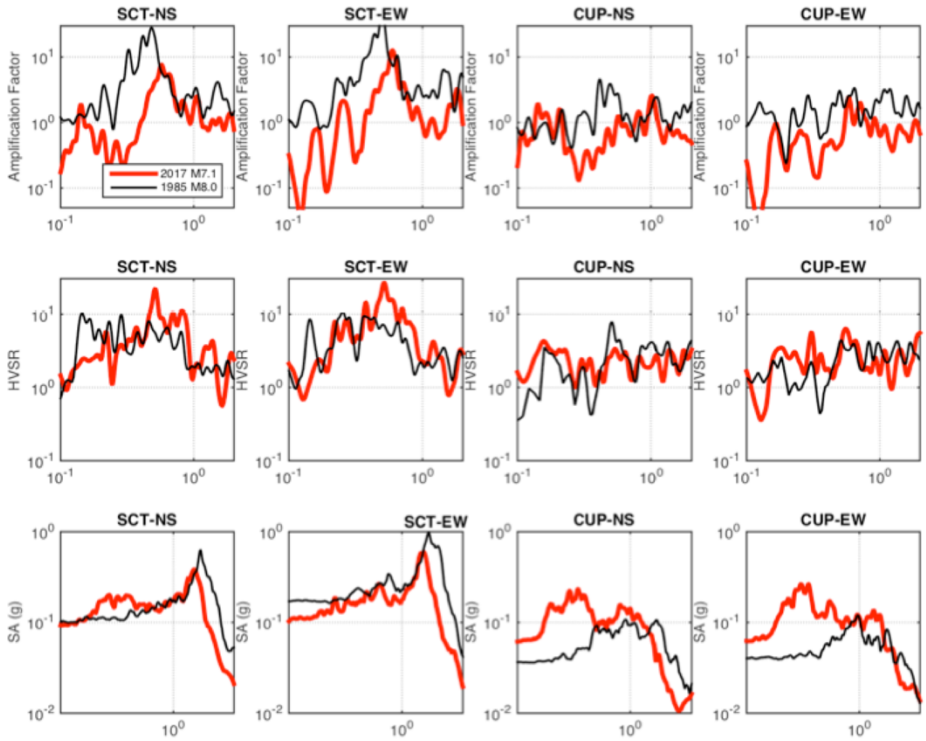

Figure 9. Spectral ratios, HVSR and spectral acceleration recorded at stations (co-located or adjacent) as captured by recordings from the 1985 and the 2017 events. (stations SCT and CUP also compared in Figure 4). Spectral ratios and HVSRs are plotted as a function of frequency [Hz]; response spectra are plotted as a function of period [sec].

ACKNOWLEDGEMENTS

The work of the GEER Association is in part supported by the National Science Foundation through the Geotechnical Engineering Program under Grant No. CMMI-1266418. This work was also partially supported under Grant No. CMMI-1822484. Any opinions, findings, and conclusions or recommendations expressed in this material are those of the authors and do not necessarily reflect the views of the NSF. Seismic records presented here were obtained by the Seismic Instrumentation Unit at the Institute of Engineering of the National Autonomous University of Mexico (UNAM) and were shared with the UNAM-GEER team prior to their public release to facilitate the reconnaissance efforts. UNAM's contribution of data as well as resources, space, and personnel to the GEER team is also hereby acknowledged.

REFERENCES

Arroyo, D., Ordaz, M., Ovando-Shelley, E., Guasch, J., Lermo, J., Pérez, C., Alcántara, L. (2011). Evaluation on the change in dominant periods in the lake-bed zone of Mexico City produced by ground subsidence.

Askar, A (1989). Wave scattering and amplification in Mexico valley, in Abstracts of the 25th General Assembly of the International Association of Seismology and Physics of the Earth Interior (IASPEI), Istanbul, 11-5, p. 408.

Campillo, M., Gariel, J. C., Aki, K., & Sanchez-Sesma, F. J. (1989). Destructive strong ground motion in Mexico city: Source, path, and site effects during great 1985 Michoacán earthquake. *Bulletin of the Seismological Society of America*, *79*(6), 1718-1735.

Cruz-Atienza, V. M., Tago, J., Sanabria-Gómez, J. D., Chaljub, E., Etienne, V., Virieux, J., & Quintanar, L. (2016). Long duration of ground motion in the paradigmatic valley of Mexico. *Scientific reports*, *6*, 38807.

Galvis F., Miranda, E., Heresi, P., Dávalos, H. and Silo, J.R. (2017). "Preliminary Statistics of Collapsed Buildings in Mexico City in the September 19, 2017 Puebla-Morelos Earthquake", Technical Report

García, D., Singh, S. K., Herraíz, M., Ordaz, M., and Pacheco, J. F. (2005). Inslab earthquakes of Central Mexico: Peak ground-motion parameters and response spectra, *Bulletin of the Seismological Society of America*, 95(6), 2272–2282.

Lermo, J., & Chávez-García, F. J. (1993). Site effect evaluation using spectral ratios with only one station, *Bulletin of the Seismological Society of America*, *83*(5), 1574-1594.

López Linares, G., Tamoa, C., Zafra, M., Gallón, A., Ruiz de Velasco, S., and Díaz Barriga, I. (2017). "Estos son los edificios que colapsaron con el terremoto en México (antes y después) - Univision." (Last accessed Sep. 26, 2017).

Margheriti, L., Wennerberg, L., & Boatwright, J. (1994). A comparison of coda and S-wave spectral ratios as estimates of site response in the southern San Francisco Bay area. *Bulletin of the Seismological Society of America*, *84*(6), 1815-1830.

Mayoral et al (2017). Geotechnical Engineering Reconnaissance of the 19 September 2017 M 7.1 Puebla-Mexico City Earthquake: Version 2.0, GEER Association, doi: 10.18118/ G6JD46

Mayoral, J.M., E. Castañon, L. Alcántara, S. Tepalcapa. (2016). Seismic response characterization of high plasticity clays. Soil Dynamics and Earthquake Engineering, Elsevier, 84, 174-189.

Ordaz, M., and Singh, S. K. (1992). "Source spectra and spectral attenuation of seismic waves from Mexican earthquakes, and evidence of amplification in the hill zone of Mexico City." Bulletin of the Seismological Society of America, 82(1), 24–43.

Ordaz, M., Miranda E. and Avilés J. (2003). "Propuesta de espectros de diseño por sismo para el DF." Revista Internacional de Ingeniería de Estructuras, 8, 189–208.

Pacheco, J. F., and Singh, S. K. (1995). "Estimation of ground motions in the valley of Mexico from normal-faulting, intermediate-depth earthquakes in the subducted Cocos plate." Earthquake Spectra, 11(2), 233–247.

Phillips, W. S., & Aki, K. (1986). Site amplification of coda waves from local earthquakes in central California. *Bulletin of the Seismological Society of America*, *76*(3), 627-648.

Rosenblueth, E., Ordaz, M., Sanchez-Sesma, F. J., and Singh, S. K. (1989). "The Mexico earthquake of September 19, 1985 - Design spectra for Mexico's Federal District." Earthquake Spectra, 5(1), 273–291.

Sánchez-Sesma, F. J., S. Chávez-Pérez, M. Sufirez, M. A. Bravo, and L. E. Pérez-Rocha (1988). On the seismic response of the Valley of Mexico, Earthquake Spectra 4, 569-589

Seed, H. B., Romo, M. P., Sun, J. I., Jaime, A., & Lysmer, J. (1988). The Mexico earthquake of September 19, 1985—Relationships between soil conditions and earthquake ground motions. *Earthquake spectra*, *4*(4), 687-729.

Servicio Sismológico Nacional. (2017). Reporte Especial: Sismo del día 19 de Septiembre de 2017, Puebla-Morelos (M 7.1). Universidad Nacional Autónoma de México (UNAM). Preliminary report, September 25, 2017, Mexico City, Mexico.

Shoja-Taheri, J., & Bolt, B. A. (1977). A generalized strong-motion accelerogram based on spectral maximization from two horizontal components. *Bulletin of the Seismological Society of America*, *67*(3), 863-876.

Singh, S. K., E. Mena, and R. Castro (1988). Some aspects of source characteristics of the 19 September 1985 Michoacán earthquake and ground motion amplification in and near Mexico City from strong motion data, *Bulletin of the Seismological Society of America* 78, 451-477.

Singh, S. K., Ordaz, M., and Pérez-Rocha, L. E. (1996). The great Mexican earthquake of 19 June 1858: Expected ground motions and damage in Mexico City from a similar future event, *Bulletin of the Seismological Society of America*, 86(6), 1655–1666.

Singh, S. K., Ordaz, M., Pacheco, J. F., Quaas, R., Alcántara, L., Alcocer, S., Gutierrez, C., Meli, R., and Ovando, E. (1999). A preliminary report on the Tehuacan, Mexico earthquake of June 15, 1999 (M = 7.0), *Seismological Research Letters*, 70(5), 489–504.

Singh, S. K., Suárez, G., and Domínguez, T. (1985). The Oaxaca, Mexico, earthquake of 1931: lithospheric normal faulting in the subducted Cocos plate, *Nature*, 317(5), 56–58.

Singh, S., L. Ponce, S. Nishenko (1985). The Great Jalisco, Mexico, earthquake of 1932: Subduction of the Rivera plate, *Bulletin of the Seismological Society of America* 75, 1301–1313.

Steidl, J. H., Tumarkin, A. G., & Archuleta, R. J. (1996). What is a reference site?, *Bulletin of the Seismological Society of America*, *86*(6), 1733-1748.

Su, F., & Aki, K. (1990). Temporal and spatial variation on coda Q^{-1} associated with the North Palm Springs earthquake of July 8, 1986. *Pure and Applied Geophysics*, *133*(1), 23-52.

Su, F., Anderson, J. G., & Zeng, Y. (1998). Study of weak and strong ground motion including nonlinearity from the Northridge, California, earthquake sequence. *Bulletin of the Seismological Society of America*, *88*(6), 1411-1425.

U.S. Geological Survey. (2017). "M 7.1 - 1km ESE of Ayutla, Mexico." (Sep. 26, 2017).

Yamamoto J., Z. Jiménez, R. Mota (1984). El temblor de Huajuapan de Leon, Oaxaca, México, del 24 de Octubre de 1980, *Geofísica Internacional* 23

Yamamoto, J., L. Quintanar, C. J. Rebollar, Z. Jiménez (2002). Source characteristics and propagation effects of the Puebla, Mexico, earthquake of 15 June 1999, *Bulletin of the Seismological Society of America* 92, 2126–2138.

Yamamoto, J., Quintanar, L., Rebollar, C. J., and Jiménez, Z. (2002). "Source characteristics and propagation effects of the Puebla, Mexico, earthquake of 15 June 1999." Bulletin of the Seismological Society of America, 92(6), 2126–2138